Stochastic resonance across bifurcation cascades

C. Nicolis
Institut Royal Météorologique de Belgique 3 av. Circulaire, 1180 Brussels, Belgium

G. Nicolis*
Interdisciplinary Center for Nonlinear Phenomena and Complex Systems, Université Libre de Bruxelles, Campus Plaine, CP 231 bd du Triomphe, 1050 Brussels, Belgium

(Received 17 January 2017; published 21 March 2017)

The classical setting of stochastic resonance is extended to account for parameter variations leading to transitions between a unique stable state, bistability, and multistability regimes, across singularities of various kinds. Analytic expressions for the amplitude and the phase of the response in terms of key parameters are obtained. The conditions for optimal responses are derived in terms of the bifurcation parameter, the driving frequency, and the noise strength.

DOI: 10.1103/PhysRevE.95.032219

I. INTRODUCTION

Stochastic resonance is a universal mechanism underlying the amplification of weak external signals by noise, as it occurs in large classes of nonlinear systems across physical, earth, and life sciences [1-3]. In its classical setting stochastic resonance is concerned with periodically forced systems subjected to noise and possessing two simultaneously stable states. In the absence of noise the periodic forcing, which is assumed to be weak, is unable to induce transitions between the states and merely modulates the instantaneous level of a relevant observable around each of them. In the absence of periodic forcing noise-driven transitions between states are taking place, but their succession is random. The presence of both forcing and noise organizes these transitions conferring to them a characteristic periodicity and enhancing, under appropriate conditions, the amplitude of the response.

Ordinarily, stochastic resonance is studied under fixed values of the parameters built in the system. There is experimental evidence [4] that varying parameters leads to shifts of the stochastic resonance optimum to different values of the noise intensity, but so far no systematic studies on the role of parameters have been reported. Now, as is well known, in nonlinear systems parameter variations typically lead to bifurcation cascades in which branches of states are annihilated and new ones emerge. In particular, situations corresponding to a unique stable state, to bistability, or to multistability may be successively realized across criticalities of various kinds [5]. The extension of the classical setting of stochastic resonance to account for such phenomena is the main objective of the present work.

The questions we raise are how the response to an external periodic forcing is affected when switching from bistability to multistability, what happens in the transition region between these different regimes, and under what conditions can the response be optimized. In previous work by one of the present authors [6] stochastic resonance in multistable systems was investigated. In this study the states were prescribed once for all and their origin was not addressed. Here we focus, rather, on how stochastic resonance perceives transitions where states are being born as the system moves across different regions in parameter space. We will be considering systems whose dynamics can be described in terms of a single variable. The particular bifurcation scenario we will be interested in is the transition from a two-state region born through a cusp-type catastrophe to a three-state one born through a butterfly-type catastrophe [7]. Transitions of this kind underlie, among others, the crystallization of several materials where intermediate metastable states are believed to be present during the nucleation stages of the process [8,9]. We stress that in addition to the (rather restricted) class of univariate systems *per se*, systems amenable to a single variable arise in more generic situations as well where, following a clear-cut separation of time scales, the evolution eventually takes place on a slow one-dimensional manifold toward which the full phase-space trajectories converge after some transient period [5].

A general formulation accounting for these features is developed in Sec. II. Section III is devoted to the response to small-amplitude forcings. We obtain analytic expressions for the amplitude and the phase of the response in terms of key parameters. The dependence of the response on these parameters is analyzed in Sec. IV and the conditions for optimal responses are derived. The low-frequency limit and the critical transition region are considered in Sec. V and the main conclusions are summarized in Sec. VI.

II. FORMULATION

Throughout this work we will be considering a one-variable nonlinear system subjected to additive periodic and stochastic forcings. The evolution of such a system can be cast in the form

$$\frac{dx}{dt} = -\frac{\partial V(x,t)}{\partial x} + F(t), \tag{1}$$

where x is the state variable, V is the potential generating the evolution, and $F(t)$ is assimilated to a Gaussian white noise of spectral intensity q^2.

We decompose the potential V as

$$V(x,t) = U(x) - \epsilon x \sin \omega t. \tag{2}$$

*Corresponding author: gnicolis@ulb.ac.be

Here, $U(x)$ is the potential in absence of the periodic forcing and ϵ, ω stand for the amplitude and frequency of the forcing, respectively. As mentioned in the Introduction, in the classical setting of stochastic resonance $U(x)$ possesses two minima (associated to two simultaneously stable steady states of the system) separated by a maximum. In the present work we aim at an extension in which, as the parameters are varied, a bistability region emanating from a supercritical pitchfork bifurcation point is gradually merging with a three stable state region emanating from a subcritical pitchfork bifurcation point and terminating with two limit point bifurcations. The simplest potential accounting for this transition is a polynomial of sixth degree encompassing cusp and butterfly-type catastrophes [7], whose full unfolding requires three control parameters. For the sake of simplicity we here limit ourselves to potentials that are even in x and require that the transition be realized by controlling a single parameter λ. A generic potential satisfying these requirements is

$$U(x) = \frac{x^6}{6} - u(\lambda_1 - \alpha\lambda)\frac{x^4}{4} - \lambda(\lambda_1 - \lambda)\frac{x^2}{2}, \tag{3}$$

where u, λ, α ($\alpha > 1$) are kept fixed and λ is varied. This potential possesses a first extremum at

$$x_0 = 0 \tag{4a}$$

and up to four additional extrema determined by the solutions of a quartic equation,

$$x_1 = -x_3 = \left\{\tfrac{1}{2}[u(\lambda_1 - \alpha\lambda) + \sqrt{u^2(\lambda_1 - \alpha\lambda)^2 + 4\lambda(\lambda_1 - \lambda)}]\right\}^{\frac{1}{2}}, \tag{4b}$$

$$x_2 = -x_4 = \left\{\tfrac{1}{2}[u(\lambda_1 - \alpha\lambda) - \sqrt{u^2(\lambda_1 - \alpha\lambda)^2 + 4\lambda(\lambda_1 - \lambda)}]\right\}^{\frac{1}{2}}. \tag{4c}$$

As can be seen, x_1 merges with x_2 and x_3 with x_4 at a value $\lambda = \lambda^*$ for which the expression within the square root vanishes. At this value the system undergoes two limit point bifurcations. In the interval $\lambda^* < \lambda < 0$ there exist then four real solutions x_1 to x_4 two of which (x_2 and x_4) merge at $\lambda = 0$ through a (subcritical) pitchfork bifurcation and disappear thereafter. In contrast, solution branches x_1 and x_3 continue in the region $0 < \lambda < \lambda_1$, merge at $\lambda = \lambda_1$, and disappear thereafter through a (supercritical) pitchfork bifurcation. Figure 1 depicts the corresponding bifurcation diagram. It can be checked straightforwardly that in absence of both the periodic forcing and the noise: x_0 is stable for $\lambda < 0$ and $\lambda > \lambda_1$ and unstable in the interval $0 < \lambda < \lambda_1$; that x_2, x_4 are unstable [maximum of $U(x)$] in the entire interval $\lambda^* < \lambda < 0$; and x_1, x_3 are stable [minimum of $U(x)$] in the entire interval $\lambda^* < \lambda < \lambda_1$.

Our aim is to analyze the response of the reference system described by the potential $U(x)$ to the periodic and stochastic forcings. As is well known, the stochastic dynamics generated by the presence of the random force $F(t)$ in Eq. (1) is a

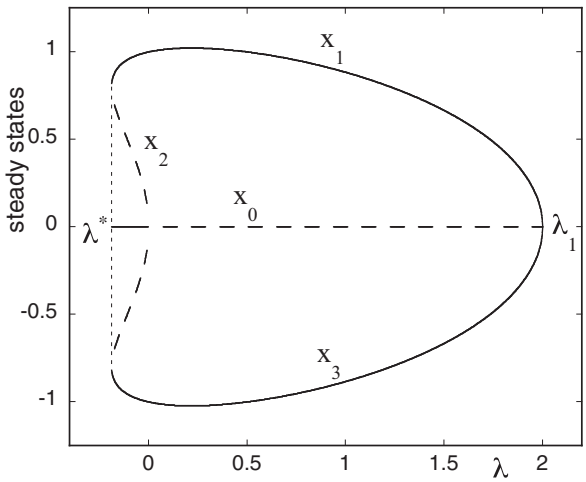

FIG. 1. Bifurcation diagram corresponding to the potential in Eq. (3) with $u = 1/2$, $\lambda_1 = 2$, and $\alpha = 3$.

diffusion process in phase space, whose probability density $\rho(x,t)$ satisfies the Fokker-Planck equation [10]

$$\frac{\partial\rho}{\partial t} = -\frac{\partial}{\partial x}\left[-\frac{\partial U}{\partial x} + \epsilon\sin\omega t)\right] + \frac{q^2}{2}\frac{\partial^2\rho}{\partial x^2} \tag{5}$$

subjected to "natural" boundary conditions (ρ along with its x-derivative vanish at $\pm\infty$). In the presence of multi-humped potentials Eq. (5) describes actually a composite process consisting of two parts:

(a) A small-scale diffusion around each of the stable states (minima of U). The characteristic time of this process is $[U''(\mathrm{st})]^{-1}$, where the accent denotes derivative of U with respect to x evaluated on a stable state.

(b) Large scale transitions between stable states across intermediate unstable states interrupting intermittently the above diffusion process, more specifically: transitions between x_1 and x_3 across x_0, for $0 < \lambda < \lambda_1$; transitions between x_1 and x_0 across x_2 as well as x_3 and x_0 across x_4, for $\lambda^* < \lambda < 0$. These transitions are activated processes whose rates depend on the respective potential barriers

$$\Delta V = \Delta U - \epsilon\Delta x\sin\omega t = U(\mathrm{unst}) - \mathrm{U(st)} - \epsilon(\mathrm{x_{unst}} - \mathrm{x_{st}})\sin\omega\mathrm{t}. \tag{6a}$$

We will be interested in situations where the characteristic time scale of process (a) is much faster than the characteristic time scales of process (b) and of the external forcing. Furthermore, the amplitude of the forcing will be assumed sufficiently weak so that no forcing-induced transition between states can take place in the absence of noise. These properties can be fulfilled provided that the parameters ω, ϵ, and q^2 satisfy the conditions

$$\omega << U''(\mathrm{st}), \quad \epsilon < \mathrm{q}^2 << \Delta\mathrm{U}. \tag{6b}$$

Now U'' as well as ΔU depend on the bifurcation parameter λ. Figures 2(a) and 2(b) summarize these dependencies in the region of positive λs. In actual fact, therefore, the bounds in Eq. (6b) are λ-dependent. For given ω, ϵ, and q^2 this requires that the system operates in a range of λ values not in the immediate vicinity of the transition points $\lambda = 0$ and $\lambda = \lambda_1$. Under the above conditions the rate of fluctuation-induced

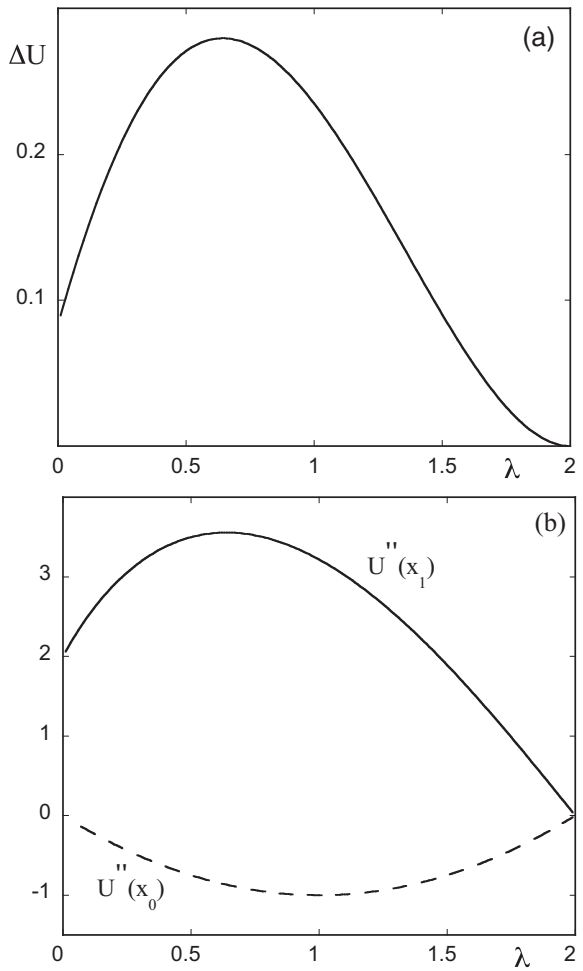

FIG. 2. Dependence on the bifurcation parameter λ in the absence of forcing, of the potential barrier ΔU (a); and of factors $U''(x_1)$ (full line) and $U''(x_0)$ (dashed line) (b). Parameter values as in Fig. 1

transitions between stable states is given by Kramers' formula [10]

$$k(t) = \frac{1}{2\pi}(|U''(\text{unst})|U''(\text{st}))^{1/2} \exp\left[-\frac{2}{q^2}\Delta V(t)\right]. \quad (6c)$$

Following previous work by the authors [1,6], one can show that in this limit Eq. (5) can be mapped into a discrete-state Markov process describing the transfer of probability masses p_i contained in the attraction basins of the stable states. In the context of the present work this leads to the following master-type equations:

A. In the $\lambda^* < \lambda < 0$ region

$$\begin{aligned}
\frac{dp_0}{dt} &= -(k_{01}+k_{03})p_0 + k_{10}p_1 + k_{30}p_3,\\
\frac{dp_1}{dt} &= k_{01}p_0 - k_{10}p_1,\\
\frac{dp_3}{dt} &= k_{03}p_0 - k_{30}p_3,
\end{aligned} \quad (7)$$

where k_{ij} denote transition rates from state i to state j. Noting that $U(x_0) = 0$, their specific forms are [cf. Eqs (6)]

$$\begin{aligned}
k_{01} &= k_1 \exp\left[\frac{2\epsilon}{q^2}x_2 \sin\omega t\right],\\
k_{03} &= k_1 \exp\left[-\frac{2\epsilon}{q^2}x_2 \sin\omega t\right],\\
k_{10} &= k_2 \exp\left[\frac{2\epsilon}{q^2}(x_2 - x_1)\sin\omega t\right],\\
k_{30} &= k_2 \exp\left[-\frac{2\epsilon}{q^2}(x_2 - x_1)\sin\omega t\right],
\end{aligned} \quad (8)$$

where

$$\begin{aligned}
k_1 &= \frac{1}{2\pi}(-\lambda(\lambda_1 - \lambda))^{1/2}|U''(x_2)|^{1/2}\exp\left[-\frac{2}{q^2}U(x_2)\right],\\
k_2 &= \frac{1}{2\pi}(U''(x_1)|U''(x_2)|)^{1/2}\exp\left[-\frac{2}{q^2}(U(x_2) - U(x_1))\right].
\end{aligned} \quad (9)$$

B. In the $0 < \lambda < \lambda_1$ region

$$\begin{aligned}
\frac{dp_1}{dt} &= -k_{13}p_1 + k_{31}p_3,\\
\frac{dp_3}{dt} &= k_{13}p_1 - k_{31}p_3
\end{aligned} \quad (10)$$

with [noting $x_0 = x_{\text{unst}} = 0$, $U(x_0) = U(\text{unst}) = 0$]

$$\begin{aligned}
k_{13} &= k \exp\left[-\frac{2\epsilon}{q^2}x_1 \sin\omega t\right],\\
k_{31} &= k \exp\left[\frac{2\epsilon}{q^2}x_1 \sin\omega t\right],\\
k &= \frac{1}{2\pi}[\lambda(\lambda_1 - \lambda)]^{1/2}(U''(x_1))^{1/2}\exp\left[\frac{2}{q^2}U(x_1)\right].
\end{aligned} \quad (11)$$

III. RESPONSE THEORY

Equations (7) and (10) define a linear system of differential equations with time-periodic coefficients. In this section we evaluate the dominant parts of the contributions of the periodic forcing to the values of p_0, p_1, and p_3 using perturbation theory. We emphasize that the response to the forcing as analyzed below pertains to the fluctuation-induced transfer of probability masses associated to each of the different stable states toward the other stable states, modulated by the presence of the external forcing. In particular, as stressed in Sec. II all processes within a particular potential well are lumped and the forcing amplitude is taken to be sufficiently weak in the sense that no forcing-induced jump between states can occur in the range of λ-values considered.

A. In the $\lambda^* < \lambda < 0$ region.

In absence of forcing $\epsilon = 0$ the steady-state solutions of Eqs. (7) read

$$\begin{aligned}
p_1^{(0)} = p_3^{(0)} &= \frac{k_1}{2k_1 + k_2} = p^{(0)},\\
p_0^{(0)} &= \frac{k_2}{2k_1 + k_2}.
\end{aligned} \quad (12)$$

We next place ourselves in the conditions where the second inequality in Eq. (6b) holds and expand the ks [Eq. (8)] in ϵ. Inserting this expansion into Eq. (7) leads to the following equations for the first order corrections δp_1 and δp_3 to $p_1^{(0)}$ and $p_3^{(0)}$:

$$\begin{aligned}\frac{d\delta p_1}{dt} &= -(k_1+k_2)\delta p_1 - k_1\delta p_3 \\ &\quad + \epsilon[\delta k_1(1-2p^{(0)}) - \delta k_2 p^{(0)}]\sin\omega t, \\ \frac{d\delta p_3}{dt} &= -k_1\delta p_1 - (k_1+k_2)\delta p_3 \\ &\quad - \epsilon[\delta k_1(1-2p^{(0)}) - \delta k_2 p^{(0)}]\sin\omega t \end{aligned} \tag{13}$$

with

$$\begin{aligned}\delta k_1 &= k_1\frac{2\epsilon}{q^2}x_2, \\ \delta k_2 &= k_2\frac{2\epsilon}{q^2}(x_2-x_1). \end{aligned} \tag{14}$$

Seeking asymptotic (long-time) solutions of Eq. (13) in the form of a superposition of $\sin\omega t$ and $\cos\omega t$ and identifying coefficients on both sides of equations leads after some straightforward calculations to

$$\delta p_1 = -\delta p_3 = R\sin(\omega t+\phi), \tag{15a}$$

where the amplitude R and phase ϕ are given by the relations

$$\begin{aligned} R &= \frac{2\epsilon}{q^2}\frac{\delta k_1(1-2p^{(0)}) - \delta k_2 p^{(0)}}{\sqrt{k_2^2+\omega^2}} \\ &= \frac{2\epsilon}{q^2}p^{(0)}x_1\frac{1}{\sqrt{1+\frac{\omega^2}{k_2^2}}}, \end{aligned} \tag{15b}$$

$$\tan\phi = -\frac{\omega}{k_2}. \tag{15c}$$

On the other hand, since $\delta p_1 = -\delta p_3$ the first-order correction to $p^{(0)}$ vanishes. To estimate the effect of the forcing on the intermediate stable state at $x_0 = 0$ we therefore need to push the expansion of the k's in Eq. (8) to the second order. Substituting into the first equation (7) leads after a straightforward calculation to

$$\begin{aligned}\frac{\delta p_0}{dt} &= -(2k_1+k_2)\delta p_0 + \frac{8\epsilon^2}{q^4}(x_2-x_1) \\ &\quad \times \frac{k_1k_2x_1}{2k_1+k_2}\frac{1}{\sqrt{1+\frac{\omega^2}{k_2^2}}}\sin(\omega t+\phi)\sin\omega t \\ &\quad + \frac{4\epsilon^2}{q^4}\frac{k_1k_2}{2k_1+k_2}x_1(x_1-2x_2)\sin^2\omega t \end{aligned} \tag{16}$$

showing that to the second order in ϵ and in the long-time limit δp_0 admits periodic solutions of the form of a superposition of $\sin 2\omega t$ and $\cos 2\omega t$ terms, plus a constant term accounting for the shift of the mean value of p_0 with respect to the zeroth order value $p_0^{(0)}$ [Eq. (12)].

B. In the $0 < \lambda < \lambda_1$ region.

In absence of forcing the steady-state solutions of Eq. (10) are simply $p_1^{(0)} = p_3^{(0)} = 1/2$. Expanding next the ks in Eq. (11) in ϵ, substituting into Eq. (10) and following the same procedure as in the previous subsection leads eventually to

$$\delta p_1 = -\delta p_3 = R\sin(\omega t+\psi) \tag{17a}$$

with

$$R = \frac{2\epsilon}{q^2}\frac{x_1}{2}\frac{1}{\sqrt{1+\frac{\omega^2}{4k^2}}}, \tag{17b}$$

$$\tan\psi = -\frac{\omega}{2k}. \tag{17c}$$

Notice that, as expressions (14), (15b), and (17b) clearly show, the actual expansion parameter conditioning the response is ϵ/q^2 rather than ϵ. In as much as q^2 is expected to be small, this shows the constructive role of noise in the amplification of the response.

It should be pointed out that the results reported in this section rest on the validity of inequalities (6b) and of the Kramers-like expressions for the transition rates [Eqs. (6c), (9), and (11)]. These expressions clearly fail in the immediate vicinity of the supercritical pitchfork bifurcation point $\lambda = \lambda_1$ and of point $\lambda = 0$ where the merging of the two- and three-state regions is occurring. In the first case the barriers ΔU separating states 1 and 3 from state 2 vanish, while in the second case the second derivative $U''(x_0)$ vanishes. The analysis of the response requires then a different approach appealing to the full Fokker-Planck equation, see Secs. IV and V.

IV. STOCHASTIC RESONANCE AND PARAMETER DEPENDENCE

Expressions (15b) and (17b), which determine the response of the system to the periodic forcing in the presence of noise in the subcritical and supercritical regions, respectively, constitute our first main result. They display a dependence on the bifurcation parameter λ, the forcing frequency ω, and the noise strength q^2 which will be analyzed in the present section. This dependence is conditioned, to a large extent, by the transition rates k_2 [Eq. (9)] and k [Eq. (11)]. For given noise strength these rates are expected to depend very sensitively on λ through both the barriers ΔU and the pre-exponential factors. Typically, they should vanish in the points of criticality λ^*, 0, and λ_1 through the second derivative of the potential, see Fig. 2(b) (critical slowing down) and present a maximum at some intermediate value of λ. This maximum results, e.g., in the supercritical case, from the competition between a maximum of ΔU and $U''(x_1)$ and a minimum of $|U''(x_0)|$. The fist two arise at a $\lambda = \lambda_1/\alpha$, the value at which the coefficient of the quartic part of the potential vanishes [cf. Eq. (3)]. The values of k_2 and k for λ values away from the maximum are expected to fall off very rapidly to practically insignificant levels. As a result, at a given λ and for values of ω substantially larger than the corresponding k values, the response is expected to be insignificant. These conjectures are fully verified by

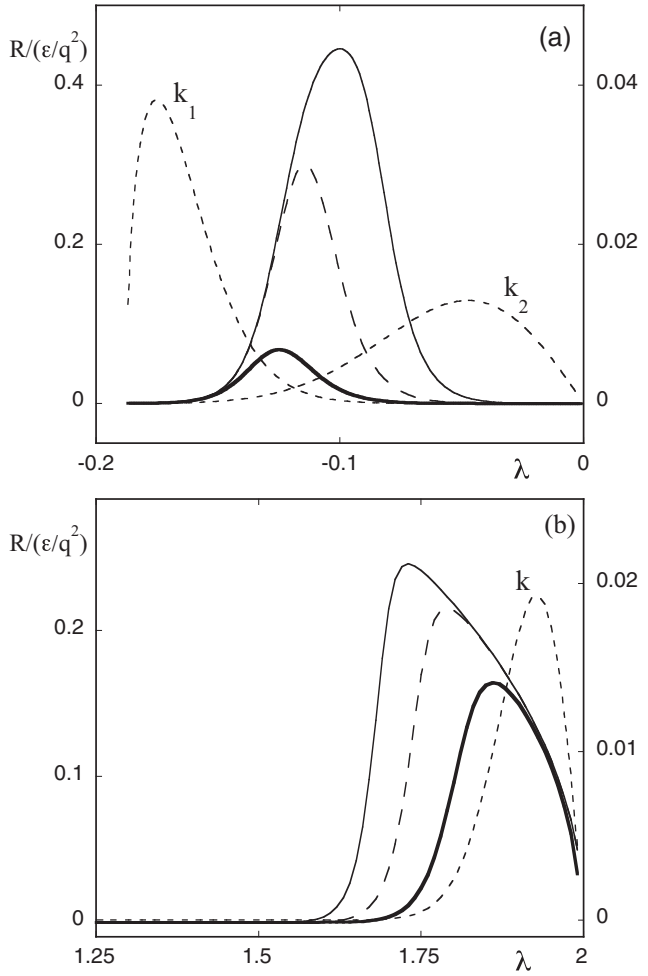

FIG. 3. Amplitude of the response (left ordinate) and corresponding values of the transition rates (right ordinate) versus the bifurcation parameter λ, in the subcritical region, Eq. (15b), (a) and the supercritical region, Eq. (17b), (b) for $\omega = 10^{-4}$ (thin full line), $\omega = 10^{-3}$ (dashed line), and $\omega = 10^{-2}$ (fat full line). Other parameters as in Fig. 1 with $q^2 = 10^{-2}$.

a detailed numerical evaluation of the expressions for the response amplitude R and the k's summarized in Figs. 3(a) and 3(b) pertaining to the subcritical and supercritical region, respectively. In both cases sharp maxima of R with respect to λ are observed, which move as ω is decreasing toward $\lambda = 0$ in Fig. 3(a) and away from $\lambda = \lambda_1$ in Fig. 3(b).

We notice that in the subcritical case the maximum response is not occurring at a λ value corresponding to the three stable states x_0, x_1, and x_3 being equally dominant [intersection point of curves k_1 and k_2 in Fig. 3(a)]. This is at first sight contrary to what might have been expected since in this "coexistence" state the values of the potential barriers separating the stable states are moderate whereas away from this value one of them is increasing, thereby slowing down substantially the corresponding transition. It highlights the important role played by the frequency of the forcing, which in a way "drives" the response toward the left or the right of the coexistence value of λ depending on whether its value tends to match the maximum of k_1 (large ω's) or of k_2 (small ω's), respectively.

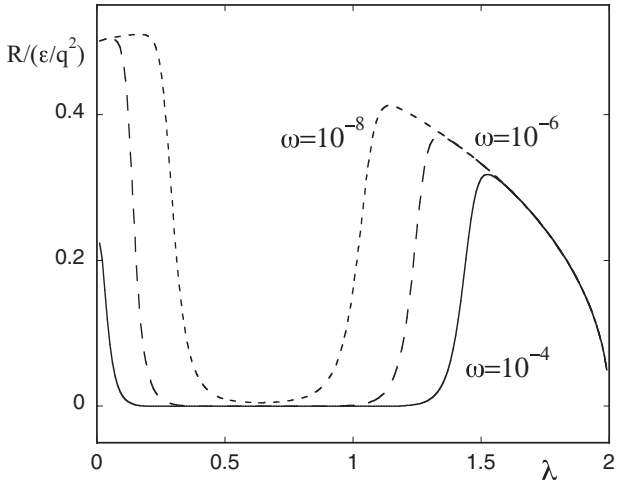

FIG. 4. As in Fig. 3(b) with smaller values of the forcing frequency and $q^2 = 0.025$.

Regarding the supercritical case, it comes as a surprise that as ω is further decreasing a second maximum of R is revealed, in the neighborhood of $\lambda = 0$. This maximum was in fact present at insignificant levels for ω values in the range depicted in Fig. 3(b), but attains values which eventually dominate those close to λ_1 for very low frequencies, matching the k values close to λ/α. As shown in Fig. 4 the two maxima are getting closer for decreasing ω's. This low frequency regime will be analyzed further in Sec. V below.

The results summarized above highlight the very pronounced selectivity of the response on the bifurcation parameter λ, for given values of the forcing frequency and noise strength. On the other hand, as seen from Eq. (4b), λ determines the "deterministic" level x_1 of the response variable x (in absence of both forcing and noise) which happens to appear explicitly in expressions (15b) and (17b) of the amplitude R of the response at the level of the probability mass p_1 around x_1. On inspecting the bifurcation diagram of Fig. 1 in conjunction with Figs. 3(a) and 3(b) one sees that responses near optimum in the subcritical region correspond to x_1 values for which in the supercritical region the response would be insignificant. Conversely, responses near optimum in the supercritical region correspond to x_1 values which are much too low and simply do not match values of stable steady states in the subcritical region. As a corollary, an optimal response R together with a high level of variable x can only be achieved if the system operates in the subcritical region.

We turn now to the dependence of the response on the noise strength, q^2. Detailed analysis of Eqs. (15b) and (17b) using expressions (8), (9), and (11) shows that the response R displays an optimum for a certain $q^2_{\max}$ whose value depends on the driving frequency ω as seen in Figs. 5(a) and 5(b) pertaining to the supercritical and subcritical cases, respectively. This property, considered to be one of the main signatures of classical stochastic resonance in a bistable system [1,3], is now shown to hold in more intricate situations as well. As can be seen the range of $q^2_{\max}$ values is more restricted in the subcritical case, indicating a higher selectivity. Furthermore, in both cases the range of $q^2_{\max}$ is more restricted as the driving frequency is lowered. Notice that $\lambda = 0$ and its close vicinity

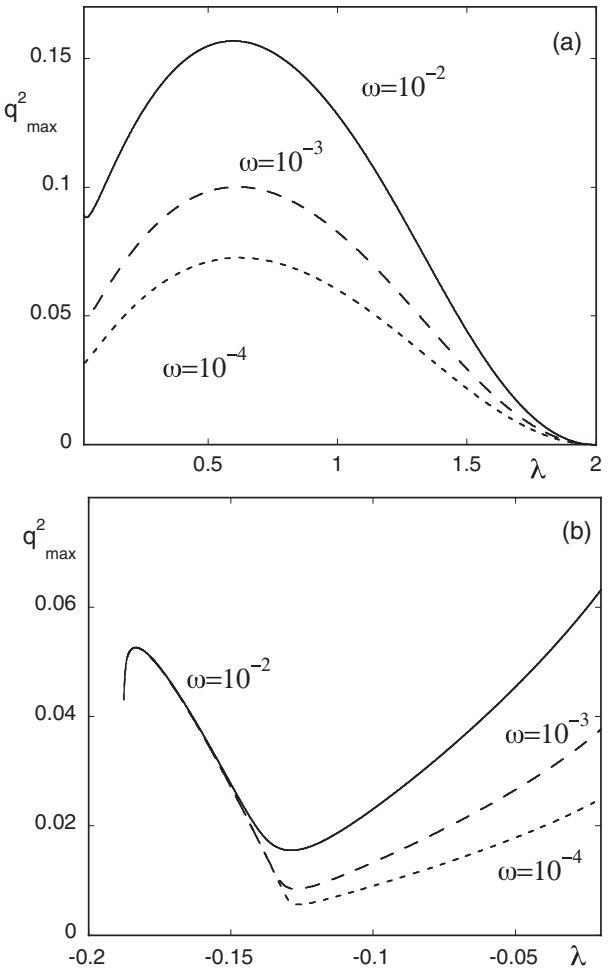

FIG. 5. Optimal values of the noise strength for which the response is maximised as a function of the bifurcation parameter λ in the supercritical region (a) and the subcritical region (b) for different values of the forcing frequency. Parameter values as in Fig. 1.

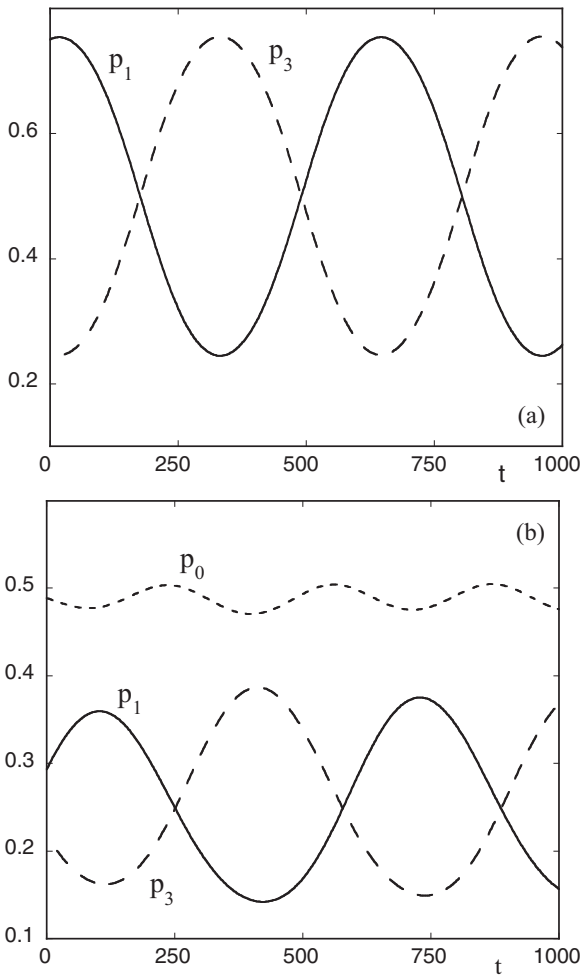

FIG. 6. Asymptotic probability masses of the corresponding attraction basins as obtained from direct numerical integration of the Fokker-Planck equation (5) in the supercritical case (a) and the subcritical case (b). Parameter values as in Fig. 1 and $q^2 = \omega = \epsilon = 10^{-2}$.

are not included in the figures since, as noticed already, the response theory in the form used here fails. This region is considered separately in Sec. V.

We close this section by summarizing the results of numerical integration of the full Fokker-Planck equation, Eq. (5). Fixing the values of ϵ, ω, and q^2 we choose values of λ corresponding to the optimal response R in the supercritical [$\lambda_{max} \approx 1.86$, see Fig. 3(b)] and subcritical [$\lambda_{max} \approx -0.12$, see Fig. 3(a)] cases, respectively. The corresponding time dependencies of the probability masses p_1 and p_3 of the supercritical case and p_1, p_3, and p_0 of the subcritical case are depicted in Figs. 6(a) and 6(b), respectively. Both the qualitative properties and the quantitative characteristics, including the amplitude R of the oscillation of, e.g., δp_1 around its average level are in very good agreement with the analytic results of Sec. III, considering also the rather high value adopted for the forcing amplitude ϵ. We notice in particular [Fig. 6(b)] that, as predicted, the response of p_0 is less pronounced and displays a periodicity half of that of p_1 or p_3. This shows the robustness of our linear response theory, as long as the system is not operating in the immediate vicinity of the transition points.

V. LOW-FREQUENCY LIMIT AND CRITICAL SLOWING DOWN

As pointed out in the end of Sec. III, the response theory based on the Kramers-like expressions of the transition rates fails in the critical region near $\lambda = 0$, where the subcritical (three stable states) and supercritical (two stable states) regimes are merging. In this section we analyze the behavior of the response in this region. We start with the full Fokker-Planck equation (5) focusing on the limit where the driving frequency ω is very small since, owing to the presence of critical slowing down, the response would otherwise be insignificant. Under these circumstances one expects that the probability density $\rho(x,t)$ will attain a "local equilibrium" with the instantaneous forcing value $\epsilon \sin \omega t$ [6,11]. The solution of Eq. (5) in this approximation reads then

$$\rho(x,t) = Z^{-1}(t) \exp\left[-\frac{2}{q^2}(U(x) - \epsilon x \sin \omega t)\right], \quad (18a)$$

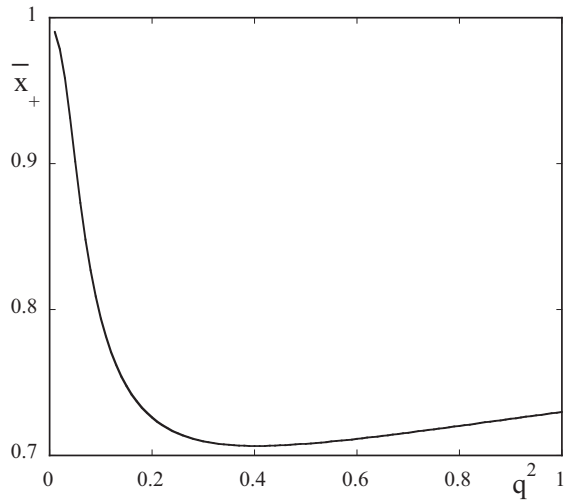

FIG. 7. One-sided average of variable x in the domain of attraction of state x_1 versus the noise strength q^2 at the critical point $\lambda = 0$ separating the two-state and three-state regimes.

where the norm $Z(t)$ is given by

$$Z(t) = \int_{-\infty}^{\infty} dx \exp\left[-\frac{2}{q^2}(U(x) - \epsilon x \sin\omega t)\right]. \quad (18b)$$

We choose to approach the limit $\lambda = 0$ from the supercritical region ($\lambda > 0$). This system possesses then two distinct stable states x_1, x_3 separated by an intermediate unstable one x_0. To evaluate the probability masses p_1, p_3 around each of these states we simply need to integrate expression (18a) in the domain of x values corresponding to their attraction basins, e.g., from 0 to ∞ for p_1. Analytic expressions can be obtained by expanding in ϵ (provided $\epsilon < q^2$) and keeping the first non-trivial term. Noticing that the first-order correction to Z vanishes by symmetry we arrive straightforwardly at the following expression for the perturbation δp_1 to p_1 caused by the forcing

$$\delta p_1 = \frac{2\epsilon}{q^2}\frac{\overline{x}_+}{2}\sin\omega t, \quad (19)$$

where $\overline{x}_+$ is the one-sided average of x in the domain of attraction $0 \leqslant x \leqslant \infty$ of x_1. A steepest descent evaluation can be carried out as long as q^2 is small with respect to the value of the barrier ΔU separating x_1 from x_0, which remains finite at and around $\lambda = 0$. It leads to $\overline{x}_+ = x_1$, i.e., to a response amplitude R merging with the one derived in Eq. (17b) in the limit where ω/k is set equal to zero. In the same limit the phase shift ψ of the response with respect to the forcing vanishes. On the other hand expression (19) remains valid in situations where the steepest descent evaluation fails, e.g., situations where the noise strength is becoming comparable to the value of the potential barrier. Exact expressions obtained at $\lambda = 0$ show that as q^2 is increasing $\overline{x}_+$ is becoming smaller than x_1, attains a shallow minimum at some critical value of q^2, and subsequently increases again (Fig. 7). In other words noise tends first to compromise the efficiency of the response, but subsequently this trend is reversed.

The low frequency limit combined with an ϵ-expansion cannot be applied straightforwardly in the vicinity of the supercritical pitchfork bifurcation point $\lambda = \lambda_1$ (as well as, in the subcritical region $\lambda < 0$, in the immediate vicinity of the two limit points at $\lambda = \lambda^*$). In these cases the noise intensity and the forcing amplitude compete directly with the distance from bifurcation. The separation between small scale diffusion around a stable state and transitions between stable states is no longer clear cut and, moreover, forcing-induced transitions between states cannot be excluded. In fact, the very mapping of Eq. (5) into a finite-state Markov process fails. To handle such situations more sophisticated perturbation analyses are necessary. Some results have been reported in the literature in cases where noise is absent [12-14], but the problem remains open when both forcing and noise are present.

On the other hand the low frequency limit and the expansion in ϵ/q^2 can be applied safely in the entire supercritical region of positive λs not in the immediate vicinity of $\lambda = \lambda_1$, leading again to expression (19). In the weak noise strength limit in which a steepest descent evaluation applies $\overline{x}_+$ is then becoming equal to x_1, indicating that the maximal response is attained at a value of the bifurcation parameter λ for which x_1 is maximum ($\lambda \approx 0.22$ for parameter values used in Fig. 1).

VI. CONCLUSIONS

Our objective in this work was to analyze how the phenomenon of stochastic resonance is modulated as a nonlinear system is moved across its bifurcation diagram. The particular bifurcation diagram we focused on (Fig. 1) pertains to the transition between a single state, two stable state, and three stable state regimes. The region of multiple states is here delimited from the single state one by super and subcritical pitchfork bifurcation points and by limit points. It takes the form of a closed loop reminiscent of isola bifurcations [15,16], the difference being that its birth is not entirely reducible to the classical isola mechanism. As a result of this closed loop structure the levels of the states in absence of noise and forcing, the potential barriers and the transition dynamics between states behave in a complex, non-monotonic fashion as the bifurcation parameter is varied, where regions of high transition rates are interrupted by regions of very low transition activity and by criticalities.

Stochastic resonance integrates these sensitivity properties by exhibiting a high selectivity of the response to the external forcing on the bifurcation parameter for given values of the driving frequency and the noise strength. Varying the driving frequency in a way to match the values of transition rates reveals optima of the response that would otherwise be masked (Figs. 3 and 4). And varying the noise strength reveals ranges of values for which the response is optimised, the optimum being, in turn, very sensitive to the values of the bifurcation parameter (Figs. 5 and 7).

Our analysis was limited deliberately to symmetric unfoldings based on a single bifurcation parameter. It would be interesting to consider stochastic resonance in the most general situation involving three parameters. Furthermore, much of the analysis can be extended to the case of traditional isolas. Contrary to our diagram of Fig. 1 the bifurcation diagram would involve here an additional branch of stable states disconnected from the isola, otherwise the system would eventually escape to infinity. Stochastic resonance would then all of a sudden be manifested in a narrow range of values of

the bifurcation parameter, those delimiting the isola itself. This could provide a potentially interesting mechanism of selective amplification and control.

ACKNOWLEDGMENTS

This work is supported, in part, by the Science Policy Office of the Belgian Federal Government.

[1] C. Nicolis, Tellus **34**, 1 (1982).
[2] R. Benzi, G. Parisi, A. Sutera, and A. Vulpiani, Tellus **34**, 10 (1982).
[3] L. Gammaitoni, P. Hänggi, P. Jung, and F. Marchesoni, Rev. Mod. Phys. **70**, 223 (1998).
[4] S. Vohra and L. Fabiny, Phys. Rev. E **50**, R2391(R) (1994).
[5] G. Nicolis, *Introduction to Nonlinear Science* (Cambridge University Press, Cambridge, 1995).
[6] C. Nicolis, Phys. Rev. E **82**, 011139 (2010).
[7] D. Saunders, *An Introduction to Catastrophe Theory* (Cambridge University Press, Cambridge, 1980).
[8] P. G. Vekilov, Cryst. Growth Des. **4**, 671 (2004).
[9] J. F. Lutsko and G. Nicolis, Phys. Rev. Lett. **96**, 046102 (2006).
[10] C. Gardiner, *Handbook of Stochastic Methods* (Springer, Berlin, 1983).
[11] M. Evstigneev and P. Reimann, Phys. Rev. E **72**, 045101(R) (2005).
[12] C. Nicolis and G. Nicolis, Phys. Rev. E **67**, 046211 (2003).
[13] M. Gitterman and G. Weiss, J. Stat. Phys. **70**, 107 (1993).
[14] S. Rosenblat and D. S. Cohen, Stud. Appl. Math. **63**, 1 (1980).
[15] M. Golubitsky and D. Schaeffer, Commun. Pure Appl. Math. **32**, 21 (1979).
[16] D. Dellwo, H. B. Keller, B. J. Matkowski, and E. L. Reiss, SIAM J. Appl. Math. **42**, 956 (1982).